vs. the P-Au-P or C-Au-C chromophores. This anomaly may possibly be explained by using detailed comparisons of the local geometry and/or extended packing.

Unambiguous confirmation of the solid-state structure was achieved by determining the crystal structure (Figure 2, Table III). As expected for most two-coordinate gold(I) complexes, the molecule is essentially linear at the gold (∠CAuP = 176.6 (6)°) as well as at the cyanide (∠NCAu = 177 (2)°). The AuP distance of 228.8 (5) ppm is similar to d(AuP) = 227.9 pm in Ph_3PAuMe[2] and d(AuP) = 225 pm in $Et_3PAuSATg$ (SATg = tetraacetylthioglucose).[19] The AuC distance of 197 (2) pm is comparable to d(AuCN) = 201 pm in $AuCN(CNCH_3)$[20] and to d(AuC) = 202 (2) pm in $4K[Au(CN)_2]\cdot K[Au(CN)_2I_2]\cdot H_2O$.[21] The large uncertainty in the bond length (d(AuC) = 212 (14)) for $KAu(CN)_2^-$ precludes any meaningful comparison with that found here.[22] The bond lengths reported for Ph_3PAuCN[1] (d(AuC) = 185 (4) pm and d(CN) = 125 (4) pm) are inconsistent with other values for gold cyanides and so are not used for comparison.[23]

The NMR and solution IR studies demonstrated that in, for example, methanol solution Et_3PAuCN (δ_P = 35.1 and δ_C = 160.4), $(Et_3P)_2Au^+$ (δ_P = 48.2), and $Au(CN)_2^-$ (δ_C = 151.4) are in equilibrium with one another. This is, to our knowledge, the first clear evidence that, even in the absence of added ligands, neutral gold(I) complexes LAuX will disproportionate. Sadler has previously demonstrated in the reaction of glutathione and Et_3PAuCl that some disproportionation occurs, generating $(Et_3P)_2Au^+$.[24] The equilibrium constant determined here is clearly solvent-dependent increasing with the polarity of the solvent. This is consistent with the formation of the ionic species $(Et_3P)_2Au^+$ and $Au(CN)_2^-$ according to eq 1.

The analogous triphenylphosphine complex Ph_3PAuCN also crystallizes in the solid state as the neutral molecular species.[1] Previous IR studies of Ph_3PAuCN in $CHCl_3$ reported only a single cyanide stretch and concluded that Ph_3PAuCN is the only species present.[9] Our ^{31}P and ^{13}C NMR results demonstrate that the complex disproportionates in solution and that the ligands exchange at a faster rate than for Et_3PAuCN. Since the ligand-scrambling reaction of Ph_3PAuCN is only observed at low temperature, there is the possibility that in other LAuX systems disproportionation may be similarly masked by rapid ligand exchange.

Labile ligand exchange is characteristic of gold(I), and it is therefore surprising that this type of disproportionation reaction has been previously overlooked or ignored. Such reactions may be very important in the biological milieu where the aqueous and therefore polar nature of intra- and intercellular compartments will facilitate similar disproportionation of gold drugs and their metabolites. It will be important to determine the effect of ligand basicity, bulk, and hydrophobicity on the extent and rate of these reactions.

Acknowledgment. A.L.H. and C.F.S. thank Smith Kline and French (SKF) for financial support and gifts of Et_3PAuCl. We acknowledge J. T. Guy and J. S. Rommel for assistance with the crystal structure, J. H. Zhang and M. J. Kwiecien for obtaining the Mössbauer spectrum, and F. Laib for obtaining the NMR spectra. A.L.H. also thanks the UMW graduate school for a graduate fellowship. W.M.R. acknowledges partial support of NSF DMR Solid State Chemistry Program Grant No. 8313710, USDOE Reactor Sharing Program Grant No. DE-FG02-80ER10770 to the MIT reactor, and SKF for funds for the purchase of the enriched Pt-source foil.

Registry No. Et_3PAuCN, 90981-41-2; Et_3PAuCl, 15529-90-5; Ph_3PAuCN, 24229-10-5; $(Et_3P)_2Au^+$, 45154-29-8; $Au(CN)_2^-$, 14950-87-9; $(Ph_3P)_2Au^+$, 47807-21-6.

Supplementary Material Available: Table of final positional and thermal parameters (1 page); table of calculated and observed structure factors (6 pages). Ordering information is given on any current masthead page.

(19) Hill, D. T.; Sutton, B. M. *Cryst. Struct. Commun.* **1980**, *9*, 679.
(20) Esperas, S. *Acta Chem. Scand., Ser. A* **1976**, *A30*, 527.
(21) Bertinotti, C.; Bertinotti, A. *Acta Crystallogr., Sect. B: Struct. Crystallogr. Cryst. Chem.* **1972**, *B28*, 2635.
(22) Rosenzweig, A.; Cromer, D. T. *Acta Crystallogr.* **1959**, *12*, 709.
(23) We thank a reviewer for pointing out that the carbon atoms in metal cyanide complxes are sometimes mislocated by crystallography.
(24) Razi, M. T.; Otiko, G.; Sadler, P. J. *ACS Symp. Ser.* **1983**, *209*, 371.

Contribution from the Laboratoire de Chimie Minérale, Université de Reims Champagne-Ardenne, F-51062 Reims, France

Dibromotris(*N*,*N*'-dimethylurea)manganese(II), a Pentacoordinated High-Spin Manganese Complex with Monodentate Ligands: Structure and Spectral Properties

Jacqueline Delaunay* and Renê P. Hugel

Received April 9, 1986

The high-spin complex dibromotris(*N*,*N*'-dimethylurea)manganese(II) crystallizes in the monoclinic system with a = 13.211 (3) Å, b = 8.670 (3) Å, c = 16.593 (4) Å, β = 106.23 (3)°, space group $C2/c$, and Z = 4. One of the characteristic features of this structure is the existence of neutral $Mn(dmu)_3Br_2$ entities (dmu = *N*,*N*'-dimethylurea), showing a distorted bipyramidal geometry with monodentate ligands, the two bromine atoms lying in equatorial positions (point group C_2). The dmu ligands are bound by oxygen atoms, but two coordinative modes are observed: axial dmu ligands are classically bonded with a Mn-O-C angle of 129.5°, whereas equatorial dmu is unusually linearly bonded with an angle Mn-O-C of 180°. This goes with a significant shortening of the Mn-O equatorial bond length compared with the axial ones. The reflectance, Raman, and infrared spectra are interpreted on the basis of these results, as well as those of its isostructural analogous $Mn(dmu)_3Cl_2$ complex. Force constants relative to MnO_3X_2 (X = Br, Cl) framework bonds have been calculated and are consistent with relative Mn-O bond length values. A d→π* metal to ligand back-donation would explain the strengthening in the equatorial Mn-O bond, the *N*,*N*'-dimethylurea ligand herein exhibiting a π-acceptor role.

Introduction

High-spin manganese(II) complexes are characterized by the absence of ligand field stabilization energy, and this has two main consequences: (i) a lower stability of manganese(II) complexes compared with those of other metals of first transition series and (ii) the possibility to obtain various coordination geometries. Nevertheless, in regard to this last point, pentacoordinated complexes of manganese(II) are not common, and hereunder we report such a case with monodentate ligands, for which a preliminary report appeared.[1]

Despite the similarity of the two urea derivative ligands as *N*,*N*'-dimethylurea (L = dmu) and *N*,*N*'-diethylurea (L = deu), two different structures for the MnL_3Br_2 stoichiometry are ob-

(1) Delaunay, J.; Kappenstein, C.; Hugel, R. *J. Chem. Soc., Chem. Commun.* **1980**, 679.

0020-1669/86/1325-3957$01.50/0

Table I. Summary of Crystal Data, Data Collection Parameters, and Least-Squares Residuals for $Mn(dmu)_3Br_2$

formula	$MnC_9H_{24}N_6O_3Br_2$
mw	479.09
cryst syst	monoclinic
space group	$C2/c$
a, Å	13.211 (3)
b, Å	8.670 (3)
c, Å	16.593 (4)
β, deg	106.23 (3)
V, Å^3	1824.8
Z	4
d_{calcd}, g·cm^{-3}	1.739
d_{measd}, g·cm^{-3}	1.74 (±0.01) (flotation method)
cryst size, mm	0.3 × 0.1 × 0.02
μ(Mo Kα), cm^{-1}	53.7
diffractometer	Philips PW 1100
radiation; λ(K$\bar{\alpha}$), Å	Mo Kα (graphite monochromated); (0.71073)
temp, °C	room temp, 20
scan method	ω–2θ
data collcn range, deg	$4 \le 2\theta \le 50$ ($-15 \le h \le +15$; $0 \le k \le 10$; $0 \le l \le 19$)
scan speed, deg·s^{-1}	0.01
scan width, deg	1.2
check reflcns	3, remeasd after every 45 reflcns (every 90 min), 400, 13$\bar{4}$, $\bar{2}$24 with a std dev <10% for intensities; cryst realigned if angular variation >0.1°
no. of unique data used	856 ($I \ge 3\sigma(I)$)
no. of params refined	97
weighting scheme	$1/\sigma^2(F_o)$
residual factors: R, R_w[a]	0.0547, 0.0513
goodness of fit indicator R_F[b]	1.82
rejected reflcns	none; $w^{1/2}\|\|F_o\| - \|F_c\|\| > 9$
largest shift/esd, final cycle (av)	0.11 (0.03)

[a] $R = \sum||F_o| - |F_c||/\sum|F_o|$; $R_w = |\sum w(|F_o| - |F_c|)^2/\sum w|F_o|^2|^{1/2}$. [b] $R_F = |\sum w(|F_o| - |F_c|)^2/(N_{observns} - N_{params})|^{1/2}$.

served. With deu, the electronic spectra[2] and the recent X-ray structure determination[3,4] indicate an ionic mixed octahedral–tetrahedral complex: $[Mn(deu)_6][MnBr_4]$. With L = dmu, the absence in the electronic spectrum of the characteristic bands of the tetrahedral $[MnBr_4]^{2-}$ anion and the results of low-temperature magnetic susceptibility and electron paramagnetic resonance spectroscopic measurements[2] suggested a mononuclear species with a distorted geometry around the manganese atom and led us to investigate the X-ray crystal structure.

Experimental Section

Preparation of $Mn(dmu)_3Br_2$. The preparation of $Mn(dmu)_3Br_2$ (white powder) has been described previously.[2] Monocrystals were obtained from a concentrated solution of the powder in dry 1-butanol and ethanol (50/50), very slowly evaporated at room temperature in a desiccator with silica gel: thin transparent plates appear after 1 month. The plates are very fragile and moisture-sensitive, and many of them were twinned. Anal. Calcd for $MnC_9H_{24}N_6O_3Br_2$: C, 22.56; H, 5.05; N, 17.54; Mn, 11.5; Br, 33.4. Found: C, 22.65; H, 5.22; N, 17.58; Mn, 11.4; Br, 33.3.

Spectra. The spectra were recorded at room temperature with the following spectrometers and methods: infrared spectrum, Perkin-Elmer Model 521 with KBr pellets (250–4000 cm^{-1}); far-infrared spectrum (20–120, 50–450, 100–700 cm^{-1}), Bruker IFS 113 V (Fourier transform) with polyethylene pellets; Raman spectrum, Coderg Model T 800 with an ionized argon laser (Coherent Radiation Model 52 B) using 250–800 mW power from the 488.0-nm line and cooled EMI 9558 QB photomultiplier for detection with the powder sample (ground crystals) introduced in a rotating cell; electronic spectrum in the visible and ultraviolet regions, Beckman UV 5240, fitted with a reflectance attachment.

Table II. Final Fractional Atomic Coordinates and Isotropic (or Equivalent) Temperature Factors (Å^2)[a]

atom	10^4x	10^4y	10^4z	B (or B_{eq}), Å^2
Br	−0521.2 (0.7)	1958.2 (1.5)	1151.2 (0.9)	3.01
Mn	0	3568.3 (2.8)	2500	2.47
O(1)	1629 (6)	3696 (9)	2460 (5)	2.49
C(1)	2193 (10)	4873 (17)	2434 (9)	3.10
N(11)	2817 (10)	5453 (13)	3147 (9)	4.73
C(11)	2981 (11)	4736 (18)	3983 (8)	4.55
N(12)	2209 (9)	5537 (13)	1717 (8)	4.01
C(12)	1671 (12)	4890 (20)	0929 (10)	5.86
O(3)	0	5915 (13)	2500	4.39
C(3)	0	7356 (21)	2500	3.43
N(31)	0319 (10)	8144 (13)	3214 (8)	5.61
C(31)	0698 (17)	7428 (20)	4024 (11)	8.16
HN(11)	3172	6329	3145	5.20
H1C(11)	2476	5139	4254	5.00
H2C(11)	3665	4965	4337	5.00
H3C(11)	2895	3646	3936	5.00
HN(12)	2576	6401	1707	5.00
H1C(12)	2137	4279	0704	6.00
H2C(12)	1344	5664	0540	6.00
H3C(12)	1129	4185	0992	6.00
HN(31)	0291	9166	3200	6.20
H1C(31)	0158	7394	4308	7.50
H2C(31)	1282	8006	4364	7.50
H3C(31)	0930	6396	3980	7.50

[a] Numbers in parentheses are the estimated standard deviations in the last significant digit.

X-ray Structure Determination. A thin plate was fixed with grease in a sealed Lindeman glass capillary and mounted on a automated diffractometer, with graphite-monochromatized Mo K$\bar{\alpha}$ radiation. The automatic searching procedure was used to find 25 reflections, which were accurately centered for determining the least-squares-refined lattice parameters.

Intensity data were collected with the ω–2θ scan technique for all nonequivalent reflections for which $4° \le 2\theta \le 50°$.[5,6] No significant change due to crystal decay was observed over the course of data collection. All other pertinent data are summarized in Table I.

Lorentz and polarization corrections were applied, but no absorption correction was made. Systematic extinctions, apart from those due to C lattice (hkl, $h + k = 2n + 1$; $h0l$, $h = 2n + 1$; $0k0$, $k = 2n + 1$), appeared for $h0l$, $l = 2n + 1$, except for two "nonobserved" reflections ($\bar{1}$0,0,3) and ($\bar{1}$0,0,11), in agreement with Cc or $C2/c$ space groups.

The observed structure factors were put on an absolute scale with a Wilson plot and led to an average B temperature factor of 2.85 Å^2 for the whole structure. The classical tests of centrosymmetry were not conclusive for the choice of the space group,[7] so we solved the structure with the less symmetric Cc space group using standard Patterson, Fourier, and least-squares methods.[8] The Patterson map gave the positions of two bromine atoms and the one manganese atom.[9] A Fourier map, calculated with the contribution of these three atoms in an asymmetric unit at four general positions (x and z coordinates of one bromine atom arbitrarily fixed at 0.0), gave the coordinates of the other 18 non-hydrogen atoms. Atomic scattering factors for neutral Mn, Br,

(2) (a) Barbier, J. P.; Hugel, R. P. *J. Inorg. Nucl. Chem.* **1973**, *35*, 781. (b) Barbier, J. P.; Hugel, R. P.; Van der Put, P. J.; Reedijk, J. *Recl. Trav. Chim. Pays-Bas* **1976**, *95*, 213.
(3) To be submitted for publication.
(4) Delaunay, J. *Structures moléculaires et propriétés spectroscopiques de composés de coordination*; Thèse d'Etat: Reims, France, May 1985.
(5) The net intensity is given as $I_{net} = I - k(F_1 + F_2)$, where I is the total count on the reflection and F_1 and F_2 are the count on each background. $k = \tau_1/(\tau_2 + \tau_2) = 3$, where τ_1 is the time spent on each reflection (120 s) and τ_2 that spent on each background (20 s).
(6) The $\sigma(I)$'s were converted to the estimated errors in the relative structure factors, $\sigma(F_o)$, by $\sigma(F_o) = 1/2(\sigma(I)/I) \times F_o$.
(7) The results of statistical tests are the following: statistical distributions related to $|E|$, average $|E^2 - 1|$, centric 0.968, acentric 0.736, result 0.858; average $|E|$, centric 0.798, acentric 0.886, result 0.823; $|E| > 1$, centric 31.7%, acentric 36.8%, result 34.8%; $|E| > 2$, centric 4.6%, acentric 1.8%, result 4.2%; the $N(Z)$ of Howells, Philipps, and Rogers gives a plot that is intermediate between the centric and acentric ones.
(8) Patterson, Fourier, and block-diagonal least-squares computations were carried out on a local IBM 1130 computer with local programs derived from those of: Laing, M. *Acta Crystallogr., Sect. B: Struct. Crystallogr. Cryst. Chem.* **1969**, *B25*, 1674.
(9) Attempts to solve the structure by direct methods with use of the MULTAN program failed (Germain, G.; Main, P.; Woolfson, M. M. *Acta Crystallogr., Sect. A: Cryst. Phys., Diffr., Theor. Gen. Crystallogr.* **1971**, *A27*, 371). Two solutions, giving the same model of two Br and one Mn, but translated in the cell, were found.

Table III. Principal Interatomic Bond Lengths (Å) and Angles (deg) in the $Mn(dmu)_3Br_2$ Asymmetric Unit[b]

	Distances[a]		
Mn–Br	2.563 (2)	O(1)–C(1)	1.271 (16)
Mn–O(1)	2.175 (8)	C(1)–N(11)	1.336 (20)
Mn–O(3)	2.035 (12)	C(1)–N(12)	1.328 (18)
O(3)–C(3)	1.249 (21)	N(11)–C(11)	1.480 (20)
C(3)–N(31)	1.331 (15)	N(12)–C(12)	1.417 (20)
N(31)–C(31)	1.438 (22)		
	Angles[a]		
Br–Mn–Br′	114.0 (4)	O(1)–Mn–O′(1)	174.2 (6)
Br–Mn–O(3)	123.0 (2)	Br–Mn–O(1)	91.6 (2)
O(1)–Mn–O(3)	87.1 (3)		
Mn–O(3)–C(3)	180	Mn–O(1)–C(1)	129.5 (8)
O(3)–C(3)–N(31)	120.9 (1.0)	O(1)–C(1)–N(11)	119.7 (1.3)
		O(1)–C(1)–N(12)	122.3 (1.2)
N(31)–C(3)–N′(31)	113.0 (2.6)	N(11)–C(1)–N(12)	118.0 (1.3)
C(3)–N(31)–C(31)	123.5 (1.3)	C(1)–N(11)–C(11)	124.3 (1.3)
		C(1)–N(12)–C(12)	121.7 (1.3)

[a] Numbers in parentheses are the estimated standard deviations in the last significant digit. [b] Atoms are labeled in agreement with Figure 1 and Table II.

C, N, O, and H were used,[10] with anomalous dispersion corrections for Mn and Br.

An initial attempt[11] to refine the structure in the space group *Cc* was unsatisfactory and led to bond lengths that should be similar being very different.[12] Consequently, we solved the structure in the space group *C*2/*c*. This involved the asymmetric unit lying on a 2-fold C_2 axis. We applied a translation of the asymmetric unit to the previously found positions.

After subsequent refinements, a difference Fourier map revealed 6 of the 12 hydrogen atoms, at a height of 0.5–0.8 e·Å^{-3}. Three of them are bonded to each nitrogen atom N(11), N(12), and N(31), with a reasonable bond length of ca. 0.9 Å and a trigonal environment of nitrogen. The three others belong to the three methyl groups and are respectively bound to C(11), C(12), and C(31). For each methyl group, we have calculated idealized positions of the two other hydrogen atoms, assuming the three hydrogen atoms uniformly located on a revolution cone with N–C–H angle of 109° 28′ and C–H bond length of 0.95 Å.[13] We have ascertained their positions in the Fourier difference synthesis (peaks of 0.3–0.7 e·Å^{-3}).

The final full-matrix least-squares refinement[14] included the 12 nonrefined hydrogen atoms (isotropic thermal *B* value of one unit higher than that of the bound atom), the 12 non-hydrogen atoms (anisotropic thermal parameters), and the scale factor. Refinement of 97 parameters, with weight $w = 1/\sigma^2(F_o)$, converged to $R = 0.0544$, $R_w = 0.0513$, and $R_F = 1.82$.[15] In the final Fourier difference synthesis, some residual peaks of about 1 e·Å^{-3} are noted between Mn and Br and between Mn and O(3). Other diffuse peaks are found around the carbon atoms C(11) and C(12) of the methyl groups, but nothing is found around C(31).

Table II lists the final atomic coordinates and isotropic (or equivalent) temperature factors. The bond distances and bond angles are given in Table III. The coordination around the manganese atom is illustrated in the ORTEP drawing (Figure 1).

Results and Discussion

Molecular Structure of $Mn(dmu)_3Br_2$. This Mn(II) complex with *N*,*N*′-dimethylurea presents a rare case of pentacoordination

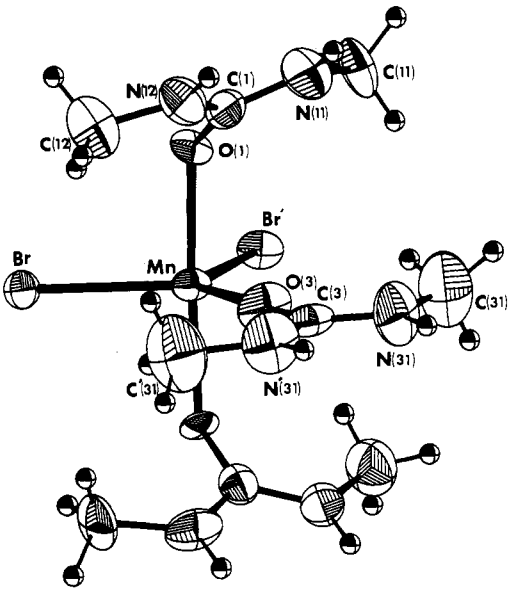

Figure 1. ORTEP model seen in perspective of the molecular $Mn(dmu)_3Br_2$ asymmetric unit.

Table IV. Assignment of Electronic Spectral Bands (10^3 cm^{-1}) of Pentacoordinated $Mn(dmu)_3Br_2$ and Analogous $Mn(dmu)_3Cl_2$

assignt	$Mn(dmu)_3Br_2$	$Mn(dmu_3)Cl_2$
$^6A'_1 \rightarrow {}^4E'$ (^4G)	19.510	
$\rightarrow {}^4A''_1 \equiv {}^4A''_2$ (^4G)	23.530	23.75
$\rightarrow {}^4A'_1 \equiv {}^4E'$ (^4G)		24.11 sh
$\rightarrow {}^4A'_2$ (^4P)	26.110	
$\rightarrow {}^4E'$ (^4D)	27.590	27.99
$\rightarrow {}^4E''$ (^4P)	28.020	
$\rightarrow {}^4A'_1$ (^4D)	29.450	
$\rightarrow {}^4E''$ (^4D)	30.675	
	36.760[a]	37.52[a]

[a] This band may be a charge-transfer band.

of manganese(II) with monodentate ligands. The coordination polyhedron is a slightly distorted trigonal bipyramid (TBP) of site symmetry C_2. In the equatorial plane, the Mn, O(3), and C(3) atoms lie on the crystallographic 2-fold axis, and the two bromine atoms are symmetrically related. The distortion of the TBP affects slightly the angle between the axial bonds (O(1)–Mn–O′(1) = 174.2 (6)°).

Pentacoordination exists for manganese(II) with quadridentate "tripodlike" ligands[16] or with porphyrins.[17] The only example, to our knowledge, of a TBP environment with monodentate ligands is $MnCl_2(2\text{-Meim})_3$ (2-Meim = 2-Methylimidazole),[18] with one chlorine atom in an axial position and one equatorial.

The axial Mn–O(1) distance of 2.175 (8) Å is normal for a bent coordinated dmu ligand (Mn–O(1)–C(1) = 129.5°), the oxygen atom sharing one lone pair with the metal atom. This is the usual way of coordination of urea and its derivatives.[19]

(10) *International Tables for X-Ray Crystallography*; Kynoch: Birmingham, England, 1962; Vol. III, pp 201–216.
(11) The function minimized was $\sum w(|F_o| - K|F_c|)^2$ where *K* is the scale factor. Anisotropic thermal parameters for bromine and manganese atoms were introduced. The weighting scheme was $w = 1$ for $F_o \leq 70$ and $w = 0.0143F_o^{-2}$ for $F_o > 70$.
(12) For example, C-N bond lengths for the two nitrogen linked to the same carbon atom were C(1)–N(11) = 1.62 Å and C(1)–N(12) = 1.07 Å and C(2)–N(21) = 1.54 Å and C(2)–N(22) = 1.23 Å. Mn–Br bond lengths were plausible, 2.54 and 2.58 Å, and angle Br–Mn–Br′ was 114°.
(13) Churchill, M. R. *Inorg. Chem.* **1973**, *12*, 1213.
(14) Final least-squares refinements in full matrix were performed on an IBM 370-168 computer (Circe, Orsay) with a local program; the ORTEP-2 thermal ellipsoid plotting program by Johnson was carried out on this computer.
(15) R_F is the so-called "*R* fit" defined by $[\sum w(|F_o| - |F_c|)^2/(m - n)]^{1/2}$, where *m* is the number of reflections (856) and *n* the number of parameters (97).
(16) Di Vaira, M.; Orioli, P. L. *Inorg. Chem.* **1967**, *6*, 955.
(17) Scheidt, W. R.; Hatano, K.; Rupprecht, G. A.; Piciulo, P. L. *Inorg. Chem.* **1979**, *18*, 292.
(18) Phillips, F. L.; Shreeve, F. M.; Skapski, A. C. *Acta Crystallogr., Sect. B: Struct. Crystallogr. Cryst. Chem.* **1976**, *B32*, 687.
(19) The M–O–C angles are found between 128° in $Cd(mu)Cl_2$ (mu = *N*-methylurea) (Nardelli, M.; Coghi, L.; Azzoni, G. *Gazz. Chim. Ital.* **1958**, *88*, 235) and 138.4° in $Ti(u)_6I_3$ (u = urea) (Davis, P. H.; Wood, J. S. *Inorg. Chem.* **1970**, *9*, 1111). The other references for urea complexes are: Nardelli, M.; Cavalca, L.; Fava, G. *Gazz. Chim. Ital.* **1957**, *87*, 1232. Haddad, S. F. Ph.D. Thesis, Fordham University, 1971. Suleimanov, Kh.; Porai-Koshits, M. A.; Antsyshkina, A. S.; Sulaimankulov. *Russ. J. Inorg. Chem.* (*Engl. Transl.*) **1971**, *16*, 1798, 3394. Figgis, B. N.; Wadley, L. G. B. *J. Chem. Soc., Dalton Trans.* **1972**, 2182. Figgis, B. N.; Wadley, L. G. B.; Graham, J. *Acta Crystallogr., Sect. B: Struct. Crystallogr. Cryst. Chem.* **1972**, *B28*, 187. Mooy, J. H. M.; Krieger, W.; Heijdenrijk, D.; Stam, C. H. *Chem. Phys. Lett.* **1974**, *29*(2), 179. Aghabozorg, H.; Palenik, G. H.; Stoufer, R. C.; Summers, J. *Inorg. Chem.* **1982**, *21*, 3903.

Table V. Vibrational Spectra of $Mn(dmu)_3X_2$ (X = Br, Cl) Complexes and Principal Force Constants in MnO_3X_2 Frameworks

1. Principal Characteristic Amide Bands of dmu in "Free" Ligand and in Complexes[a]

	dmu		$Mn(dmu)_3Br_2$		$Mn(dmu)_3Cl_2$	
	Raman	IR[b]	Raman	IR	Raman	IR
str ν(C=O) (+δ(N—H), amide I band		1620 vs, br	1639 vw	1629 vw, br	1638 vw	1628 vs, br
			1660 sh		1660 sh	
		(1670 vs)				
str ν_{as}(C—N) + bend δ(N—H), amide II band				1508 m		1510 m
		1528 sh	1522 vw		1525 vw	
			1562 sh		1557 sh	
	1584 vw	1574 m	1584 vw	1582 vw	1585 vw	1582 vw
		(1560 vs)				
out-of-plane δ(C=O) def				752 w		754 m
		770 vw	787 vw	774 w	778 sh	774 m
					798 vw	

2. Principal Internal Valence Force Constants f in MnO_3X_2 Frameworks (X = Br, Cl) (in Approximation of Trigonal Bipyramid C_{2v})

	f, mdyn·Å^{-1}		
	Mn–O_{eq}	Mn–O_{ax}	Mn–X
$Mn(dmu)_3Br_2$	2.72	2.22	1.11
$Mn(dmu)_3Cl_2$	2.68	2.22	1.00

[a] vs = very strong, m = medium, w = weak, vw = very weak, br = broad. [b] In parentheses are spectral bands of solutions in $CHCl_3$ (Nujol suspension).[2]

The same mode of coordination is found in the *N,N'*-diethylurea (deu) complex with the same stoichiometry, which was shown[4] to be ionic ($[Mn(deu)_6][MnBr_4]$) with an average Mn–O distance of 2.20 Å. Similar Mn–O distances are also observed in octahedral manganese(II) complexes with organic ligands.[20-22] In a TBP environment, Mn–O distances of 2.03, 2.06, and 2.28 Å have been found in a zeolite compound.[23]

The equatorial Mn–O(3) bond length of 2.035 (12) Å (with a Mn–O(3)–C(3) angle of exactly 180°) is significantly shorter than the axial ones and refers to a previously unobserved alternative linear coordination mode of dmu. Moreover, the equatorial dmu is particularly flat in comparison with the axial ones.[24] In the former, the thermal ellipsoid of oxygen O(3) shows that the major principal axis of displacement is directed perpendicular to the Mn–O(3) bond in the urea plane,[25] depending on the coordination mode of dmu. However, the three dmu ligands have a syn-syn conformation,[26] in agreement with previous infrared studies.[27]

A possible explanation of the linear coordination, never seen before, may arise from the electronic structure of the planar dmu ligand. Beside the classical structure with two lone pairs on the oxygen, explaining the angular coordination, dmu may also exist with an electronic structure similar to that of formaldehyde, although in the latter, the C–O bond is particularly short.[28] In this case, if we consider the dmu lying in the *xy* plane and C(3), O(3), and Mn on the *y* axis, one lone pair on oxygen remains nonbonding in the *x* direction and the other is *y* directed, consistent with a linear coordination to the metal.

Another factor contributing to the overall effect is the π-acceptor capacity of the ligand. Such ligands, according to some authors, favor the TBP geometry.[29,30] Here the planarity[31] of the dmu ligand would involve a π-acceptor capacity, increased by the presence of good π-donor bromine atoms in the same plane. So, a possible metal to ligand d→π^* back-bonding (between the d_{yz} orbital of the metal and the π^* LUMO of the ligand) can contribute to the shortening of the bond. The band at 36 760 cm^{-1} in the electronic spectrum (vide infra) might be assigned to this charge transfer.

Hydrogen-bonding contacts are few and weak. Distances Br---N (3.46–3.67 Å) could be considered as weak hydrogen bonds with usual criterion,[32] the strongest being observed between Br and HN(31) for the same *z* coordinate, probably leading to an increased stability of the equatorial dmu position. Moreover, an empty channel between sheets of $Mn(dmu)_3Br_2$ molecules, parallel to *ab* plane, agrees with the very thin plate-shaped crystals.

Electronic Reflectance Spectra of $Mn(dmu)_3X_2$ (X = Cl, Br). Reflectance spectra of high-spin pentacoordinated manganese(II) complexes exhibit weak absorption bands. The spectra of $Mn(dmu)_3Br_2$ and of isostructural $Mn(dmu)_3Cl_2$[33] are given in Figure 2. The well-resolved bands of the former have been assigned according to Ciampolini and Mengozzi's energy level diagram,[34] established for D_{3h} complexes of the $3d^5$ configuration, taking into account different parameters (geometrical and various ligands). These are the following for the MnO_3Br_2 chromophore: ligand field parameter $Dq = 0.6 \times 10^3$ cm^{-1} (intermediate between octahedral MnO_6, $Dq \simeq 0.8 \times 10^3$ cm^{-1}, and $MnBr_6$, $Dq \simeq 0.6 \times 10^3$ cm^{-1}, and tetrahedral $MnBr_4$, $Dq \simeq 0.3 \times 10^3$ cm^{-1});[35] γ

(20) Glowiak, T.; Ciunik, Z. *Bull. Acad. Pol. Sci., Ser. Sci. Chim.* **1977**, *25*(4), 277.
(21) L'Haridon, P.; Le Bihan, M. T.; Laurent, Y. *Acta Crystallogr., Sect. B: Struct. Crystallogr. Cryst. Chem.* **1972**, *B28*, 2743.
(22) Lis, T. *Acta Crystallogr., Sect. C: Cryst. Struct. Commun.* **1983**, *C39*, 39.
(23) Yanagida, R. Y.; Vance, T. B.; Seff, K. *Inorg. Chem.* **1974**, *13*, 723.
(24) The least-squares planes of the OCNN urea skeleton and atomic deviations therefrom, as well as dihedral angles giving dmu conformations, are given in Table SIV in supplementary material. The N(31)–C(31) bond departs 1.15° from the OCNN plane in the equatorial dmu, whereas the N(11)–C(11) and N(12)–C(12) bonds depart about 6°.
(25) Angles (in degrees) between the major axis of the ellipsoid of a few atoms and bonds are given in Table SII in supplementary material.
(26) Nomenclature taken up here is from "syn-periplanar" and "anti-periplanar" (Eliel, E. L.; Allinger, N. L.; Angyal, S. J.; Morrison, G. A. *Conformational Analysis*; Interscience: New York–London–Sydney, 1967; p 10) giving the position of CH_3 in dmu in comparison with that of the C=O carbonyl group.
(27) trans–trans conformation after: Mido, Y. *Spectrochim. Acta, Part A* **1972**, *28*, 1503.
(28) Harris, D. C.; Bertolucci, M. D. *Symmetry and Spectroscopy*; Oxford University Press: New York, 1978.
(29) Chastain, B. B.; Rick, E. A.; Pruett, R. L.; Gray, H. B. *J. Am. Chem. Soc.* **1968**, *90*, 3994.
(30) Basolo, F.; Pearson, R. G. *Mechanisms of Inorganic Reactions*; Wiley: New York–London–Sydney, 1967.
(31) Gerloch, M.; Hanton, L. R.; Manning, M. R. *Inorg. Chim. Acta* **1981**, *48*, 205.
(32) Intermolecular contacts are given in Table SIII in supplementary material. The Van der Waals radii sum is $r_{Br} + r_N = 3.45$ Å: Hamilton, W. C.; Ibers, J. A. *Hydrogen Bonding in Solids*; Benjamin: New York–Amsterdam, 1968.
(33) The lattice spacings (*d*, Å) of the powder diffraction patterns of $Mn(dmu)_3X_2$ (X = Br, Cl, I) are very similar, and these compounds are considered isostructural (see supplementary material).
(34) Ciampolini, M.; Mengozzi, C. *Gazz. Chim. Ital.* **1974**, *104*, 1059.

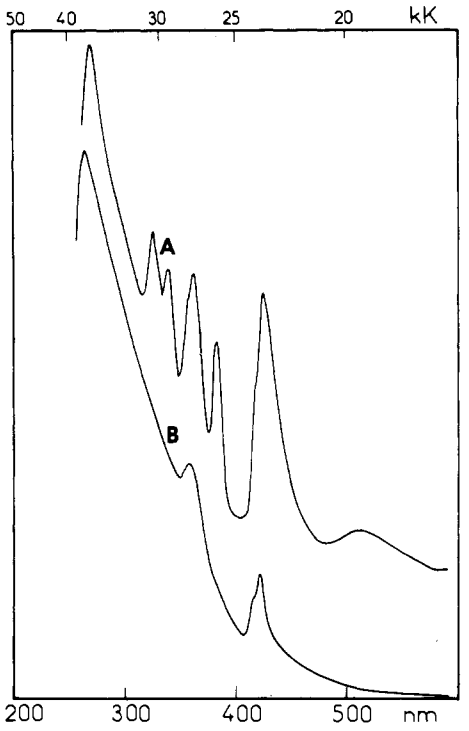

Figure 2. Reflectance spectra of $Mn(dmu)_3Br_2$ (A) and of $Mn(dmu)_3Cl_2$ (B).

$= Dq_{ax}/Dq_{eq} = 1.2$, where Dq_{eq} is a weighted average for (2Br + 1O) Dq values; nephelauxetic ratio $\beta = 0.86$ for the proposed diagram is an acceptable value for our complex.[35] The assignments of reflectance spectra are given in the Table IV.

Infrared and Raman Spectra of $Mn(dmu)_3X_2$ (X = Br, Cl). The spectra of $Mn(dmu)_3Br_2$ and of isostructural $Mn(dmu)_3Cl_2$ have been assigned. Shifts by complex formation of the dmu ligand bands have been observed, particularly for the characteristic amide bands (Table V1). The comparison of the CO stretching band in the "free" dmu ligand with that in the Mn(II) complexes shows about a 40-cm^{-1} decrease of the ν(C=O) stretching vibration frequency (amide I band). Coordination of dmu through the oxygen atom is further accompanied by an increase of around 22 cm^{-1} of the frequency of the asymmetric stretching vibration ν_{as}(C—N) (amide II band). These shifts are consistent with the presence of resonant forms $^{+}N{=}C{-}O^{-}$, suggesting conformations of methylamino groups more favorable for π-electron delocalization. Appearance of weak multiple bands, found in Raman spectra of complexes and missing in the dmu spectrum, accounts for both effects, on ν_{as}(C—N) and δ(N—H), of dissymmetrical angular and of linear C—O→Mn bonds. These effects were shown up by the splitting of equal intensity (IR) of the band due to the out-of-plane (OCNH) bending of the C=O group: δ_{op}(C=O). One of the components is slightly shifted (+4 cm^{-1}) relative to that of the "free" ligand, whereas the other is shifted by around −17 cm^{-1}. The former, much less affected by coordination, is probably due to the equatorial dmu molecule, for which the linear bonding involves some rigidity, and the latter would be due to the axial dmu one.

Infrared and Raman spectra in the low-frequency range (0-700 cm^{-1}) have been assigned in terms of skeletal (metal–ligand) vibrations. A normal-coordinate analysis of the skeletal part of the $Mn(dmu)_3Br_2$ complex (MnO_3X_2, X = Br, Cl; local symmetry $D_{3h} \rightarrow C_{2v}$) has been performed[3,4] in order to obtain an approximate satisfactorily general valence force field. The 12 vibration modes have been assigned by using spectra of some octahedral complexes:[4] $Mn(dmu)_6(ClO_4)_2$, $Cd(deu)_6(ClO_4)_2$, $Mn(u)_6Br_2$ (u = urea), and the mixed octahedral–tetrahedral $[Mn(deu)_6][MnBr_4]$ complex. For the sake of brevity, we only report hereafter the bands observed for Mn–X and Mn–O stretching modes, using the mass effect of halogens for the former. Therefore, the bands at 210–220 cm^{-1} (X = Br) and 248–266 cm^{-1} (X = Cl) are respectively assigned to symmetrical ν_s(Mn–X) and asymmetrical ν_{as}(Mn–X) metal–halogen stretching modes, as it was found for other distorted trigonal-bipyramidal compounds.[36] In the Raman spectra of $Mn(dmu)_3X_2$, the band at 618, 613 cm^{-1} (X = Br, Cl), missing in those with dmu ligand and of octahedral complexes, refers to the stretching mode of the particular manganese to equatorial oxygen bond, ν_s(Mn–O_{eq}). Stretching vibration frequencies of manganese to axial oxygen bonds are found around 520 and 570 cm^{-1} (respectively symmetrical and asymmetrical), values close to those found for an octahedral MnO_6 framework and an identical angular bonding way of deu ligand in $[Mn(deu)_6][MnBr_4]$.[3,4]

Internal valence force constants for the framework vibrations of $Mn(dmu)_3X_2$ have been deduced from the symmetry force constant calculations (F matrix).[3] The most interesting ones refer to Mn–O_{eq} and Mn–O_{ax} bonds (Table V2). The calculated values are very similar in the two complexes with a systematically larger one for Mn–O_{eq}, related to its shortness, compared with the axial one.

Acknowledgment. We thank Dr. Cl. Pascard (Gif-sur-Yvette) for the data collection on an automated diffractometer, Professor M. Manfait (Reims) for Raman spectra records, and Professor A. Alix (Reims) for help in force constant calculations.

Registry No. $Mn(dmu)_3Br_2$, 75657-77-1.

Supplementary Material Available: Perspective view of packing in the unit cell and listings of anisotropic thermal parameters and root mean square displacements for non-hydrogen atoms, intermolecular contacts with principal angles between $Mn(dmu)_3Br_2$ asymmetric units, least-squares planes of the OCNN urea skeleton and dihedral angles giving N,N'-dimethylurea conformations, and lattice spacings for $Mn(dmu)_3X_2$ (X = Br, Cl, I) (6 pages); tables of calculated and observed structure factors (5 pages). Ordering information is given on any current masthead page.

(35) Jorgensen, C. K. *Oxidation Numbers and Oxidation States*; Springer Verlag: Berlin, 1969. According to this author, nephelauxetic ratio β (=1 − h(ligand) × k(central ion)) is 0.84 and 0.92 for octahedral $MnBr_6$ and MnO_6, respectively.

(36) Bamfield, P.; Price, R.; Miller, R. G. *J. Chem. Soc. A* **1969**, 1447.